arXiv:1404.4144v1 [cond-mat.stat-mech] 16 Apr 2014

January 16, 2022

Interacting particles in a periodically moving potential: Traveling wave and transport

Rakesh Chatterjee[1], Sakuntala Chatterjee[2,*], Punyabrata Pradhan[2,*], and S. S. Manna[2]
[1] *CMP Division, Saha Institute of Nuclear Physics, 1/AF Bidhan Nagar, Kolkata 700064, India*
[2] *Department of Theoretical Sciences, S. N. Bose National Centre for Basic Sciences, Block - JD, Sector - III, Salt Lake, Kolkata 700098, India*

We study a system of interacting particles in a periodically moving external potential, within the simplest possible description of paradigmatic symmetric exclusion process on a ring. The model describes diffusion of hardcore particles where the diffusion dynamics is locally modified at a uniformly moving defect site, mimicking the effect of the periodically moving external potential. The model, though simple, exhibits remarkably rich features in particle transport, such as polarity reversal and double peaks in particle current upon variation of defect velocity and particle density. By tuning these variables, the most efficient transport can be achieved in either direction along the ring. These features can be understood in terms of a traveling density wave propagating in the system. Our results could be experimentally tested, e.g., in a system of colloidal particles driven by a moving optical tweezer.

PACS numbers: 05.70.Ln, 05.40.-a, 05.60.-k, 83.50.Ha

The advent of state-of-the-art technique to maneuver colloidal particles using laser field has opened up new avenues of research [1–5]. Recently, single colloidal particle in a periodically moving optical potential has been used to experimentally investigate several important aspects [6–9] of nonequilibrium systems. However, far less explored is the situation where colloidal particles, subjected to such a time-periodic potential, can also interact with each other. Though the crucial role of interaction has been studied intensively in the past for nonequilibrium steady states [10–12], not much is known about driven many-particle systems having a time-periodic steady state where macroscopic properties are a periodic function of time.

In this paper, we ask what happens when a system of interacting colloidal particles is driven by time-periodic forces. Do the particles always show directional motion? What are the conditions for the optimum transport? These questions are relevant not only to the colloidal particles, but are also important in the context of stochastic pumps [13–15] and thermal ratchets [16–19] as well as driven fluids in general [20, 21], e.g., in microfluidic devices [22] manipulated by time-varying forces.

We address these questions in a setting of paradigmatic exclusion processes [23] where we consider the simplest possible interaction among the particles, viz. hardcore repulsion, which is present in almost all systems due to excluded volume effects and especially important for dense packing of particles. The model is defined on a one dimensional periodic lattice of L sites, each of which can be occupied by at most one particle. The effect of a periodically moving external potential is modeled as a moving disorder or defect with the diffusive dynamics modified locally at the defect site which travels along the lattice with a uniform velocity v and with a residence time $\tau = 1/v$ at each site. A particle hops to its empty nearest neighbor with the following rates: (i) $p/2$ from the defect site, (ii) $r/2$ to the defect site and (iii) $q/2$ otherwise (see Fig. 1). A configuration of the system is specified by occupancy $\{\eta_i^{(\alpha)}\}$ of each site and position of the defect site α at a given time, where the occupancy $\eta_i^{(\alpha)}$ of the i-th site takes the value 1 (0) if the site is occupied (empty).

Despite its apparent simplicity, the model exhibits strikingly rich transport properties arising solely due to the hardcore exclusion among the particles. Since time-averaged applied force, due to the external potential, at any site is zero, it is not a priori clear if the system can support a current and, if so, in which direction. We find that there is indeed a nonzero current and remarkably the current reverses its direction and even shows positive and negative peaks, as the defect velocity v and the particle density ρ are varied. By tuning v and ρ, the most efficient transport can be achieved in either direction along the ring. Interestingly, the moving defect gives rise to a traveling wave density pattern in the system, which however always travels in the direction of the defect movement. Unlike the perturbative approach used in [15, 24, 25], we consider the case when the disorder is strong. In this limit, our analytical theory predicts the exact structure of the density wave, which explains the above results.

For $v = 0$, the model describes an equilibrium system with an external potential V_0 present only at the defect site. From the detailed balance condition, the density at the defect site $\sim \exp(-\beta V_0)$ where $V_0 = \beta^{-1} \ln(p/r)$ and β inverse temperature. The densities at the other sites are uniform. An infinitely large potential barrier corresponds to $r = 0$.

For nonzero defect velocity, we consider a strongly driven system with a large potential barrier where the

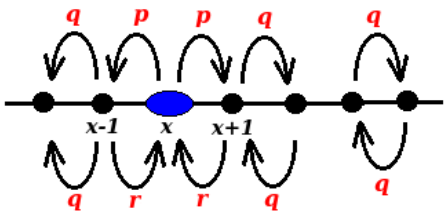


FIG. 1: (Color online) Schematic diagram of the model. At a particular time, the defect site is at x and marked by an oval shape. Other sites are shown as black solid circles. Transition from (to) the defect site takes place with rate p (rate r). All other transitions take place with rate q. The transition from a particular site takes place only if the site is occupied and the destination site is empty.

relaxation dynamics down (up) the barrier is much faster (slower) than that in the bulk and also the defect velocity is much larger than the bulk relaxation rate, implying $p, v \gg q \gg r$. For simplicity, we throughout consider infinite barrier, i.e., $r = 0$ and, without any loss of generality, one can set $p = 1$.

We first consider the limit $q = 0$ which means that at any given time, the particle can move if and only if its position coincides with the position of the defect site at that time [28]. This limit is important since, as we see later, it provides insights into the case with nonzero q. Starting from a random initial configuration, the system eventually settles into a time-periodic steady state where the density-profile has the form of a traveling wave moving around the system with the same speed v as that of the defect. From now on, unless stated otherwise, we carry out all our measurements precisely at the time-steps $t = n\tau$ when the moving defect, after spending the residence time τ at a site, is about to move on to the next one, with $n = 0, 1, \ldots \infty$. Note that it is not easy to determine the time-periodic steady state for all time t. However, the analysis becomes much simpler for time $t = n\tau$ when one writes down the following descrete-time evolution equation for density $\rho_i^{(\alpha)}(t) = \langle \eta_i^{(\alpha)}(t) \rangle$,

$$\langle \rho^{(\alpha+1)}(t+\tau)| = \langle \rho^{(\alpha)}(t)|\mathcal{W}^{(\alpha+1)}. \tag{1}$$

Here $\langle \rho^{(\alpha)}(t)| \equiv \{\rho_1^{(\alpha)}(t), \ldots \rho_i^{(\alpha)}(t), \ldots, \rho_L^{(\alpha)}(t)\}$ is a row-vector of length L, with i-th element being $\rho_i^{(\alpha)}(t)$ and $\mathcal{W}^{(\alpha)}$ is the transition matrix with the defect site at α. The conditional probability that, given the defect site is occupied, the site exchanges particle with its right (left) neighbor during the time-interval τ is denoted as a_+ (a_-). For $q = r = 0$, non-vanishing transition rates are found only at the site α and hence one can explicitly construct the transition matrix in terms of a_+ and a_-. We have an expression for these quantities starting from the microscopic dynamics:

$$a_+ = \left[\frac{\langle \eta_\alpha^{(\alpha)} \eta_{\alpha+1}^{(\alpha)} (1 - \eta_{\alpha+2}^{(\alpha)}) \rangle}{\kappa_1 \langle \eta_{\alpha+1}^{(\alpha)} \rangle} + \frac{\langle (1 - \eta_\alpha^{(\alpha)}) \eta_{\alpha+1}^{(\alpha)} (1 - \eta_{\alpha+2}^{(\alpha)}) \rangle}{2\kappa_2 \langle \eta_{\alpha+1}^{(\alpha)} \rangle} \right] \tag{2}$$

$$a_- = \left[\frac{\langle (1 - \eta_\alpha^{(\alpha)}) \eta_{\alpha+1}^{(\alpha)} \eta_{\alpha+2}^{(\alpha)} \rangle}{\kappa_1 \langle \eta_{\alpha+1}^{(\alpha)} \rangle} + \frac{\langle (1 - \eta_\alpha^{(\alpha)}) \eta_{\alpha+1}^{(\alpha)} (1 - \eta_{\alpha+2}^{(\alpha)}) \rangle}{2\kappa_2 \langle \eta_{\alpha+1}^{(\alpha)} \rangle} \right] \tag{3}$$

where the density at the defect site α decays, following a Poisson process with rates $1/\kappa_1(v) = [1 - \exp(-p/2v)]$ and $1/\kappa_2(v) = [1 - \exp(-p/v)]$, depending on the occupancy of the neighboring sites (see Appendix A for details). The transition matrix can now be written as

$$\begin{aligned}
\mathcal{W}_{i,j}^{(\alpha+1)} &= (1 - a_+ - a_-) \qquad \text{for } i = j = \alpha + 1, \\
\mathcal{W}_{i,j}^{(\alpha+1)} &= 1 \qquad \text{for } i = j \neq \alpha + 1, \\
\mathcal{W}_{i,j}^{(\alpha+1)} &= a_+ \qquad \text{for } i = \alpha + 1 \text{ and } j = \alpha + 2, \\
\mathcal{W}_{i,j}^{(\alpha+1)} &= a_- \qquad \text{for } i = \alpha + 1 \text{ and } j = \alpha.
\end{aligned}$$

In the long time limit, the time-periodic structure of the steady state implies that the density profile comes back to itself after each complete cycle of the defect movement around the ring, i.e., $\mathcal{W}^{(\alpha)}\mathcal{W}^{(\alpha+1)} \ldots \mathcal{W}^{(L)}\mathcal{W}^{(1)} \ldots \mathcal{W}^{(\alpha-1)}$ has an eigenvector $\langle \rho_{st}^{(\alpha)}|$, with eigenvalue unity. Then the ith element $\rho_{st,i}^{(\alpha)}$ of $\langle \rho_{st}^{(\alpha)}|$, i.e., steady-state density at site i, satisfies

$$\rho_{st,i}^{(\alpha+1)} = \rho_{st,i-1}^{(\alpha)}. \tag{4}$$

To solve for the density profile in the time-periodic steady state, we note that, at the time of measurement, the defect site α registers a lower density compared to the bulk because, for $r = 0$, particles cannot hop in to the defect site but can only hop out. Similarly, as $q = 0$, the neighboring sites ($\alpha \pm 1$) can only receive particles from the defect site but they cannot lose particles. The site $(\alpha + 1)$ thus has a density higher than that at the bulk. On the other hand, the site $(\alpha - 1)$, which could have only lost a particle in the previous time step when the defect was at $\alpha - 1$, now can receive a particle from the defect site α and brings its density back to the bulk level. Therefore, regarding the structure of the density profile as a function of position, we formulate an ansatz in the form of a traveling density wave which moves with the defect site α:

$$\begin{aligned}
\rho_{st,i}^{(\alpha)} &= \rho_- \qquad \text{for } i = \alpha, \\
\rho_{st,i}^{(\alpha)} &= \rho_+ \qquad \text{for } i = \alpha + 1 \\
\rho_{st,i}^{(\alpha)} &= \rho_b \qquad \text{otherwise.}
\end{aligned} \tag{5}$$

For example, $\langle \rho_{st}^{(1)}| = \{\rho_-, \rho_+, \rho_b, \ldots, \rho_b\}$ for $\alpha = 1$. The ansatz can be used in Eqs. 1 and 4, to obtain

$$\rho_+ a_+ + \rho_b = \rho_+, \tag{6}$$

$$\rho_+ a_- + \rho_- = \rho_b, \tag{7}$$

which can be solved by using particle-number conservation $\rho_+ \rho_- + (L - 2)\rho_b = L\rho$ to get the exact densities

$$\rho_b = \frac{(1 - a_+)L}{2 - a_+ - a_- + (1 - a_+)(L - 2)} \rho \simeq \rho, \tag{8}$$

$$\rho_+ = \frac{1}{1-a_+}\rho_b \simeq \frac{1}{1-a_+}\rho, \tag{9}$$

$$\rho_- = \frac{1-a_+-a_-}{1-a_+}\rho_b \simeq \frac{1-a_+-a_-}{1-a_+}\rho, \tag{10}$$

as $L \gg 1$. Note that, we have obtained the density profile in terms of $a_\pm(\rho, v)$ which depend on the global density ρ and the defect velocity v, and involve three-point correlations as in Eqs. 2 and 3. From Eqs. 9 and 10, it immediately follows that $\rho_+ > \rho$ and $\rho_- < \rho$, i.e., a bump and a trough are formed respectively in front of the defect site and at the defect site. In a many-particle system, due to the lack of closure in time-evolution equations for correlation functions (BBGKY hierarchy), it is often difficult to obtain such a general structure of the density as a function of position. Therefore, it is quite remarkable that we obtain an exact structure of the density profile for this system. Interestingly, using a dynamic density functional theory, a traveling density wave of similar structure has been found in a system driven by a moving external potential [20, 21].

To obtain the current, we note that only the two bonds adjacent to the defect site can contribute to the current, since no hopping takes place across any other bond. As the defect visits a particular site with rate v/L the current is $J_0(\rho, v) = \frac{v}{L}\langle \eta^{(\alpha)}_{\alpha+1}\rangle(a_+ - a_-)$ which can be written in terms of $\rho_\pm$,

$$J_0(\rho, v) = \frac{v}{L}(\rho_+ + \rho_- - 2\rho), \tag{11}$$

after inverting Eqs. 9, 10 and substituting $\langle \eta^{(\alpha)}_{\alpha+1}\rangle = \rho_+$. The current is nonzero in general as $a_+ \neq a_-$ or $(\rho_+ - \rho) \neq (\rho - \rho_-)$ from Eqs. 6 and 7.

So far, we have only discussed the general properties of density profile and current using exact expressions. Now we obtain explicit functional dependence of $a_\pm(\rho, v)$ on ρ and v within mean-field theory, where the three point correlations in Eqs. 2 and 3 are assumed to be factorized. Therefore, we get

$$a_+ = (1-\rho)\left[\rho_-(1-e^{-p/2v}) + \tfrac{(1-\rho_-)(1-e^{-p/v})}{2}\right] \tag{12}$$

$$a_- = (1-\rho_-)\left[\rho(1-e^{-p/2v}) + \tfrac{(1-\rho)(1-e^{-p/v})}{2}\right] \tag{13}$$

Using the above mean field expression for $a_\pm$ into Eqs. 9 and 10, the following quadratic equation can be obtained for ρ_-,

$$\begin{aligned}(\rho_- - \rho)\{1 - (1-\rho)(\rho_-\omega_1 + (1-\rho_-)\omega_2)\} \\ +\rho(1-\rho_-)\{\rho\omega_1 + (1-\rho)\omega_2\} = 0\end{aligned} \tag{14}$$

where $\omega_1 = 1/\kappa_1(v) = [1 - \exp(-p/2v)]$ and $\omega_2 = 1/2\kappa_2(v) = [1 - \exp(-p/v)]/2$. Out of the two possible solutions, only one is physically relevant as the other one is larger than unity. The solution for ρ_- now can be used, in Eqs. 12 and 13, to find $a_\pm$ and then ρ_+ from Eq. 9. The solutions for $\rho_\pm$ take a particularly simple form in the limit of large v where we expand ω_1 and ω_2 in the leading order of $1/v$ to obtain

$$\rho_+ = \frac{2v\rho}{2v - (1-\rho)p} \tag{15}$$

$$\rho_- = \frac{\rho(2v - 2p + p\rho)}{2v - p} \tag{16}$$

The mean-field expression of current can be obtained, using Eqs. 12 and 13, as

$$J_0(\rho, v) = \frac{v}{L}(1 - e^{-p/2v})\rho_+(\rho_- - \rho). \tag{17}$$

Interestingly, the current always flows in the direction opposite to the defect movement since $\rho_- < \rho$. This counter-intuitive result can be qualitatively explained in the following way. The positive current $\rho_+(1-\rho)$ across the bond $(\alpha, \alpha+1)$ and the negative current $\rho_+(1-\rho_-)$ across the bond $(\alpha-1, \alpha)$ is due to the diffusive flux from the bump to the bulk and from the bump to the trough, respectively. Clearly, the net current is negative. As shown later, this feature survives even for generic q and ρ. Substituting the previously obtained expressions for ρ_+ and ρ_- in Eq. 17, the current can be written as a function of ρ and v.

To check the above analytical results, we perform Monte Carlo simulations with $p = 1$ (see Appendix B for details). We show the variation of $\rho_\pm$ as a function of ρ and v in Figs. 2(A) and 2(B), respectively, for $q = 0$ (red squares). The analytical results (lines) show excellent agreement with the simulations. We present simulation results (red squares) for current as a function of ρ and v in Figs. 3(A) and 3(B), respectively, again in good agreement with analytical results (red solid line). Expectedly, for very low and high densities, the current is vanishingly small for any finite v. The current reaches a negative peak at an intermediate density, different from half filling, thus manifesting the absence of particle-hole symmetry. Similar non-monotonic variation of current is observed as v is varied for a fixed ρ. For small $v \ll 1$, $\rho_\pm$ are independent of v and therefore current $J_0 \sim v$. For large $v \gg 1$, it can be straightforwardly shown, by using Eqs 15 and 16, that $J \sim 1/v$. These plots show that it is possible to choose the defect velocity and the particle density to optimize the transport in the system in the direction opposite to defect motion.

For nonzero q, we do not have any closed form analytical solution of Eq. 1. However, it can be shown from the microscopic dynamics that the density profile $\rho(x, t)$ satisfies the diffusion equation

$$\frac{\partial \rho}{\partial t} = D\frac{\partial^2 \rho}{\partial x^2} \tag{18}$$

with boundary condition for current $-D\partial\rho/\partial x = \rho_+ v$ at $x = vt$ where the diffusion coefficient $D = q/2$. The

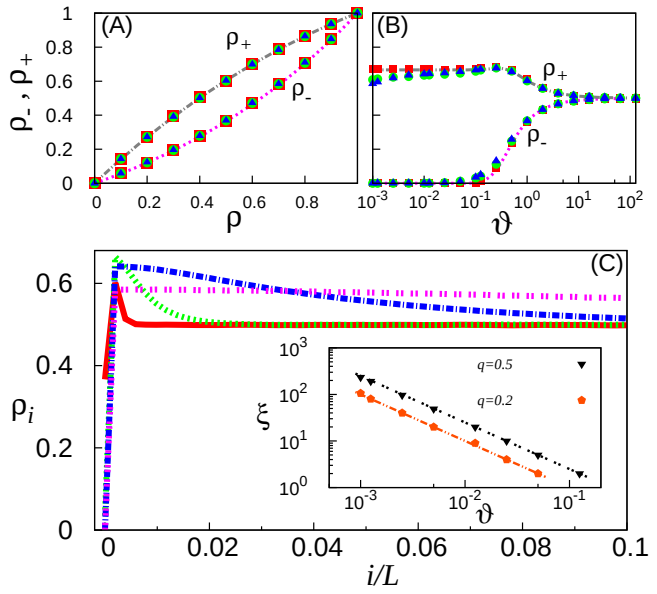


FIG. 2: (Color online) ρ_+ and ρ_- are plotted against global density ρ with $v = 1$ in panel (A) and against the defect velocity v with $\rho = 0.5$ in panel (B), for $q = 0$ (red squares), 0.2 (green circles) and 0.5 (blue triangles). Analytical prediction for ρ_+ (ρ_-) is shown by grey (pink) dashed-dotted (dotted) lines. In panel (C), densities from simulations are plotted against scaled distance (scaled by a factor $1/L$) from the defect site for $v = 1.0$ (red solid), 0.1 (green single-dotted), 0.01 (blue dashed-dotted) and 0.001 (pink double-dotted) with $q = 0.5$. Inset in panel (C) shows the variation of ξ against v for $q = 0.2$ and 0.5 (dotted lines - analytical predictions). Throughout we use $L = 512$, $p = 1$, $r = 0$.

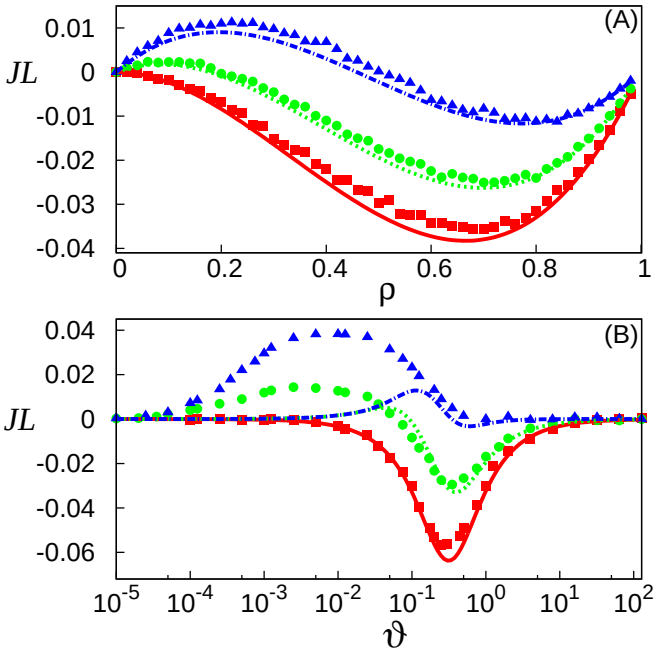


FIG. 3: (Color online) Scaled current (scaled by a factor L) is plotted against density ρ for $v = 1$ in panel (A) and against defect velocity v for $\rho = 0.5$ in panel (B) for $q = 0$ (red squares), 0.2 (green circles), 0.5 (blue triangles); in both the panels, $p = 1$, $r = 0$ and $L = 512$. Analytical results for $q = 0, 0.2$ and 0.5 are shown by red solid, green dotted and blue dashed-dotted lines, respectively.

density profile $\rho(x,t)$ then has the solution

$$\rho(x,t) = \rho_+ e^{-(x-vt)/\xi} + \rho, \tag{19}$$

with $\xi = D/v$. In Fig. 2(C), we plot the density as a function of x and, in the inset, the length-scale ξ as a function of v, which agrees remarkably well with the above form of $\xi(v)$. In other words, for large v when the defect movement is much faster compared to the other relaxation time scales, ξ is small and the structure of the density profile remains almost same as in the case of $q = 0$, i.e., there is a bump (ρ_+), a trough (ρ_-) and almost uniform bulk-density. However, for small v, ξ becomes large and the density profile shows extended spatial structure. Naturally, the description of density profile in terms of only bump and trough does not remain valid anymore.

For large v, to a good approximation, $\rho_\pm$ remains independent of q (see Fig. 2(A)). To calculate the current in mean-field approximation, we note that, for $q \neq 0$, the following three bonds contribute to the current during the time-interval τ. The mean-field current across the bond between sites $\alpha-1$ and α is $\tilde{q}[\rho(1-\rho_-)-\rho_-(1-\rho)]$, between sites α and $\alpha+1$ is $-\tilde{p}\rho_+(1-\rho_-)$ and between sites $\alpha+1$ and $\alpha+2$ is $\tilde{p}\rho_+(1-\rho)$. For large v, the effective rates $\tilde{p} = (v/L)(1-e^{-p/2v})$ and $\tilde{q} = (v/L)(1-e^{-q/2v})$ are the hopping probabilities from the defect and the bulk site, respectively, to the unoccupied nearest neighbor during the residence time τ. Therefore we obtain the net current

$$J_q(\rho, v) \simeq \tilde{p}\rho_+(\rho_- - \rho) + \tilde{q}(\rho - \rho_-). \tag{20}$$

Clearly, the first term is always negative, and the second term is always positive. The competition between these two terms results in interesting effects like polarity reversal of current as ρ and v are varied. In Fig. 3(A), the current is plotted as a function of ρ. Evidently, there is no particle-hole symmetry and current switches sign as a function of ρ, with a positive and a negative peak in the current-density plot. We obtain quite good agreement between our mean-field predictions and simulations. Small discrepancies can be attributed to the presence of spatial correlations in the system.

In Fig. 3(B), current is plotted as a function of v for various values of q. One striking aspect in this plot is the noticeable variation of current over almost five decades of v. For large $v \gg 1$, current decays as $1/v$, as follows from a straightforward analysis of Eq. 20 where one expands $\rho_\pm$, $\tilde{p}$ and $\tilde{q}$ in leading order of $1/v$. For

intermediate values of v, current shows polarity reversal, i.e., for any nonzero q and $0 < \rho < 1$, there exists a $v_c(q,\rho)$ such that $J > 0$ for $v < v_c$ and $J < 0$ for $v > v_c$. Moreover, for any given ρ and non-zero q below a particular value, there are positive and negative peaks of current at particular values of v, indicating that most efficient transport can be achieved in either direction along the ring. Our analytical results capture these broad features quite well. Particularly, for large v, the agreement between the expression in Eq. 20 and simulation is excellent. However, the quantitative agreement between analytical results and simulations is not good when v becomes small. The closed form expression for ρ_+ at large v does not remain valid anymore and therefore cannot be used to obtain the current in this regime. In the equilibrium limit of $v \to 0$, one must have $\rho_+ \to \rho$, which is indeed the case in simulations. However, as seen from Fig. 2C, the decay of ρ_+ is extremely slow, e.g., for $q = 0.5$, over two decades of v, ρ_+ decays approximately by a factor of only two.

It should be possible to design experiments where our model can be realized. For example, colloidal suspension of micron-sized beads, naturally having excluded volume interaction, can be confined in a narrow channel and acted on by a moving optical tweezer, which constitutes a relevant experimental set up. For a typical colloidal particle of diameter $a = 1\mu m$, suspended in an aqueous solution at room temperature, we obtain self-diffusion constant $D \sim 0.4\mu m^2 s^{-1}$ using Stoke-Einstein relation and the characteristic diffusive time-scale $4a^2/D \sim 2.5s$. Our model with $q = 0.4s^{-1}$ and packing fraction $\rho = 0.5$, predicts the optimum velocity of the tweezer $v \sim 2\mu m s^{-1}$ for most efficient transport in the opposite direction.

In this paper, we propose a minimal but a non-trivial model to study an interacting-particle system driven by a potential barrier moving on a ring. We find that the particle-current has interesting nonmonotonic dependence on the velocity v of the moving barrier and particle density ρ. Most remarkably, the current reverses its direction and even shows positive and negative peaks as v and ρ are varied separately. We have also obtained the condition for the optimum transport of particles, which can be achieved in both directions along the ring. Our analysis can be applied to the cases of a finite barrier ($r \neq 0$), a moving potential well ($r > p$) or multiple defects and could also be useful in systems with a more complex form of interaction among the particles [26]. From a more general perspective, our study provides important insights into the nature of transport in interacting-particle systems having a time-periodic steady state.

Appendix A: Calculation of $a_\pm$ for $q = r = 0$

As defined in the main text, a_+ is the conditional probability that given the defect site is occupied, the particle from the defect site hops to its right neighbor. We use the notation $\hat{1}$ to denote an occupied defect site and $\hat{0}$ for an empty defect site. If a particle in the defect site has to hop to its right neighbor, then the possible local configurations are $1\hat{1}0$ and $0\hat{1}0$. In the first case, the move takes place if the defect site is chosen and the particle decides to jump to the left. The probability that this happen in the first time-step dt is $pdt/2$ where we discretize time in steps of infinitesimal interval dt with $Ldt = 1$ and $L \gg 1$. If it happens in the second infinitesimal time-step, then in the first time-step the jump did not happen (which has a probability $(1 - pdt/2)$. Therefore the probability that the jump takes place in the second time-step is

$$\left(1 - \frac{pdt}{2}\right)\frac{pdt}{2}. \tag{A-1}$$

Similarly, the probability that the jump takes place in the third time-step is

$$\left(1 - \frac{pdt}{2}\right)^2\frac{pdt}{2}, \tag{A-2}$$

and so on. Thus, the probability that the rightward jump from the defect site takes place in any of the τ/dt time-steps ($\tau = 1/v$ the residence time of the defect) is given by

$$\frac{pdt}{2}\left[1 + \left(1 - \frac{pdt}{2}\right) + \left(1 - \frac{pdt}{2}\right)^2 + \ldots + \left(1 - \frac{pdt}{2}\right)^{\tau/dt}\right] = \frac{pdt}{2}\frac{1 - (1 - pdt/2)^{\tau/dt-1}}{1 - (1 - pdt/2)} = \left(1 - e^{-p/2v}\right) \tag{A-3}$$

Using similar arguments, one can show that, for the local configuration $0\hat{1}0$, the probability that the rightward jump from the defect site takes place in any of the τ/dt time-steps is $(1-\exp(-p/v))/2$. Therefore the expression for a_+ becomes

$$a_+ = \left[\frac{\langle \eta_\alpha^{(\alpha)}\eta_{\alpha+1}^{(\alpha)}(1 - \eta_{\alpha+2}^{(\alpha)})\rangle}{\kappa_1\langle \eta_{\alpha+1}^{(\alpha)}\rangle} + \frac{\langle (1 - \eta_\alpha^{(\alpha)})\eta_{\alpha+1}^{(\alpha)}(1 - \eta_{\alpha+2}^{(\alpha)})\rangle}{2\kappa_2\langle \eta_{\alpha+1}^{(\alpha)}\rangle}\right] \tag{A-4}$$

In a similar way, the expression for a_- can also be derived.

The structure of the rate matrix $\mathcal{W}$ depends on the position of the defect site α and its elements can be written in terms of $a_\pm$. For example, when $\alpha = 1$, the matrix is

$$\mathcal{W}^{(1)} = \begin{bmatrix} (1 - a_+ - a_-) & a_+ & 0 & \ldots & 0 & a_- \\ 0 & 1 & 0 & 0 & \ldots & 0 \\ \ldots & \ldots & \ldots & \ldots & \ldots & \ldots \\ \ldots & \ldots & \ldots & \ldots & \ldots & \ldots \\ 0 & \ldots & 0 & 0 & 1 & 0 \\ 0 & 0 & \ldots & 0 & 0 & 1 \end{bmatrix}$$

and for $\alpha = 2$

$$\mathcal{W}^{(2)} = \begin{bmatrix} 1 & 0 & 0 & \dots & 0 & 0 \\ a_- & (1-a_+-a_-) & a_+ & 0 & \dots & 0 \\ 0 & 0 & 1 & 0 & \dots & 0 \\ \dots & \dots & \dots & \dots & \dots & \dots \\ 0 & \dots & 0 & 0 & 1 & 0 \\ 0 & 0 & \dots & 0 & 0 & 1 \end{bmatrix}.$$

Appendix B: Simulation Details

The Monte Carlo simulations have been performed using the following algorithm with random sequential update rules. We start with an initial configuration where N randomly chosen sites of a periodic lattice of sixe L are filled with particles. Initially we chose a particular site as the defect site which has a different hopping rate than the rest of the system. In Fig. 1, the oval shaped site is the defect site and p, q, r are the hopping rates for different sites. We perform the following steps repeatedly in the simulations.

Step 1 - A site is chosen at random and updated as per the transition rates shown in Fig. 1. A single Monte Carlo step (MCS) is defined as L such update trials.

Step 2 - The defect site moves on the lattice with velocity v, i.e., the defect stays at a particular site for a residence time $\tau = 1/v$ MCS. After τ MCS, the defect moves to the next site.

After the system reaches the time-periodic steady state, the quantities such as density profile, $\rho_\pm$ and particle current are measured.

[1] A. Ashkin, Phys. Rev. Lett. **24**, 156 (1970); A. Ashkin, J. M. Dziedic, J. E. Bjorkholm and S. Chu, Opt. Lett. **11**, 288 (1986).

[2] A. Simon and A. Libchaber, Phys. Rev. Lett. **68**, 3375 (1992); L. P. Faucheux, G. Stolovitzky, and A. Libchaber, Phys. Rev. E **51**, 5239 (1995).

[3] G. Volpe, L. Helden, T. Brettschneider, J. Wehr, and C. Bechinger, Phys. Rev. Lett. **104**, 170602 (2010).

[4] R. F. Service, Science **282**, 399 (1998). H. Gau, S. Herminghaus, P. Lenz, and R. Lipowsky, Science **283**, 46(1999). A. Terray, J. Oakey, and D. W. M. Marr, Science **296**, 1841 (2002). A. Yethiraj and A. van Blaaderen, Nature **421**, 513 (2003).

[5] W. Hess and R. Klein, Adv. Phys. **32**, 173 (1983). C. Bechinger and E. Frey, J. Phys.: Condens. Matter **13** 321 (2001). G. L. Hunter and E. R. Weeks, Rep. Prog. Phys. **75**, 066501 (2012).

[6] V. Blickle, T. Speck, L. Helden, U. Seifert and C. Bechinger, Phys. Rev. Lett. **96**, 070603 (2006).

[7] V. Blickle, T. Speck, C. Lutz, U. Seifert and C. Bechinger, Phys. Rev. Lett. **98**, 210601 (2007).

[8] D. Andrieux, P. Gaspard, S. Ciliberto, N. Garnier, S. Joubaud, and A. Petrosyan, Phys. Rev. Lett. **98**, 150601 (2007).

[9] J. R. Gomez-Solano, A. Petrosyan, S. Ciliberto, R. Chetrite, and K. Gawedzki, Phys. Rev. Lett. **103**, 040601 (2009).

[10] T. Chou, K. Mallick and R. K. P. Zia, Rep. Prog. Phys. **74**, 116601 (2011).

[11] I. Buttinoni, J. Bialke, F. Kummel, H. Lowen, C. Bechinger, and T. Speck, Phys. Rev. Lett. **110**, 238301 (2013).

[12] F. Kummel, B. ten Hagen, R. Wittkowski, I. Buttinoni, R. Eichhorn, G. Volpe, H. Lowen, and C. Bechinger, Phys. Rev. Lett. **110**, 198302 (2013).

[13] S. Rahav, J. Horowitz, and C. Jarzynski, Phys. Rev. Lett. **101**, 140602 (2008).

[14] V. Y. Chernyak and N. A. Sinitsyn, Phys. Rev. Lett. **101**, 160601 (2008).

[15] K. Jain, R. Marathe, A. Chaudhuri, and A. Dhar, Phys. Rev. Lett. **99**, 190601 (2007).

[16] F. Marchesoni, Phys. Rev. Lett. **77**, 2364 (1996).

[17] U. Seifert, Phys. Rev. Lett. **106**, 020601 (2011).

[18] P. Reimann, Phys. Rep. **361**, 57 (2002).

[19] N. Golubeva and A. Imparato, Phys. Rev. Lett. **109**, 190602 (2012).

[20] F. Penna and P. Tarazona, J. Chem. Phys. **119**, 1766 (2003).

[21] P. Tarazona and U. M. B. Marconi, J. Chem. Phys. **128**, 164704 (2008).

[22] T. M. Squires and S. R. Quake, Rev. Mod. Phys. **77**, 977 (2005).

[23] I. Liggett, *Interacting Particle Systems* (Springer-Verlag, Berlin, 1985).

[24] R. Marathe, K. Jain, and A. Dhar, J. Stat. Mech. P11014 (2008).

[25] D. Chaudhuri and A. Dhar, Europhys. Lett. **94** 30006 (2011)

[26] R. Chatterjee, S. Chatterjee and P. Pradhan, *in preparation.*

[27] N. Rajewsky, L. Santen, A. Schadschneider, and M. Schreckenberg, J. Stat. Phys. **92**, 151 (1998).

[28] For small v and $q = 0$, an interesting connection exists between the model and a symmetric exclusion process with *site-wise* ordered sequential update [26] where sites are updated consecutively one after another in a particular direction along the ring. Note that this ordered sequential update rule is different from those studied in the past [27].